

# PRELIMINARY RESULTS OF ION TRAJECTORY TRACKING IN THE ACCELERATION REGION OF THE VINCY CYCLOTRON

by

Andjelija Ž. ILIĆ, Jasna L. RISTIĆ-DJUROVIĆ, and Saša T. ĆIRKOVIĆ

Received on March 10, 2006; accepted in revised form on April 30, 2006

In an accelerating region of a cyclotron, an ion makes a large number of turns; thus, its tracking requires fast as well as highly accurate computation. A computer code based on the Runge-Kutta method of the fourth order with the adaptive time step has been developed. The accuracy requirement is simultaneously set on position and momentum calculation. Magnetic fields, used as inputs, have been evaluated in terms of the radial fluctuations of the orbital frequency, *i. e.* their isochronisms. Ion trajectory tracking has been performed for the following four test beams:  $H^-$ ,  $H_2^+$ ,  $^4He^+$ , and  $^{40}Ar^{6+}$ .

*Key words:* cyclotron, ion beam, trajectory tracking, adaptive time step, magnetic fields, isochronism

## INTRODUCTION

In cyclotron design and beam dynamics analysis, it is common to treat separately the central, acceleration and extraction regions. This is because each of these regions imposes different requirements and challenges. In the acceleration region, ions travel through an isochronized magnetic field, tracing a spiral orbit. A very large number of turns are performed, resulting in a substantial trajectory length. As a consequence, the crucial requirement is to improve computational speed while preserving high accuracy, along the long numerically integrated trajectory. The VINDY software package, primarily tailored to accommodate extraction region beam dynamics and analysis, has been developed previously, as shown in [1, 2]. It has a modular structure and is organized in such a manner as to enable easy adjustments and implementation in similar beam dynamics problems. A beam trajectory in the extraction region is several hundreds times shorter than the one in the acceleration re-

gion. Also, in the extraction region, a beam trajectory is shaped solely by the magnetic field, while in the acceleration region the fundamental, *i. e.* accelerating effect, comes from the electric field. The elaborate code changes necessary to address these two differences were made and, as a consequence, the newly developed part of the VINDY package intended for beam dynamic simulations in the acceleration region, arose from the extraction region portion of the package. Note that the acceleration region part of the VINDY package could be easily applied to the central region as well, if the numerically calculated electric field maps are used as an input and if the procedures describing the obstacles in the central region (such as posts) are integrated with the rest of the code. Our goal is to describe the simulation and analysis method and assess its efficiency. The results of the simulation for the four test beams are given as an illustration of the trajectory tracking computational method.

## THE VINCY CYCLOTRON

The VINCY Cyclotron [3] is a multipurpose machine whose function is to accelerate light and heavy ions with specific charges ranging from  $\eta = 0.15$  to  $\eta = 1$ . The cyclotron magnet has four straight sectors per pole, a pole diameter of 2 m, a sector-to-sector gap of 36 mm, and a valley-to-valley gap of 190 mm. The maximum magnetic induction in the machine center is 1.97 T.

Scientific paper  
UDC: 621.039:539...17  
BIBLID:1451-3994, 21 (2006), 1, pp. 29-33

Authors' address:  
VINČA Institute of Nuclear Sciences  
Laboratory of Physics (010)  
P. O. Box 522, 11001 Belgrade, Serbia

E-mail address of corresponding author:  
jasna@stanfordalumni.org (J. L. Ristić-Djurović)

The isochronized magnetic fields in the median plane used as input are calculated according to Gordon's procedure [4, 5] and based on the measured magnetic field maps, as well as on the simulated magnetic field maps obtained using MERMAID – the finite element software package [6].

The test ion beams of the VINCY Cyclotron are 65 MeV H<sup>-</sup>, 30 MeV per nucleon H<sub>2</sub><sup>+</sup>, 7 MeV per nucleon <sup>4</sup>He<sup>+</sup>, and 3 MeV per nucleon <sup>40</sup>Ar<sup>6+</sup> beams. These four ion beams have been chosen to check the four acceleration regimes, employing acceleration with harmonic numbers 1, 2, 3, and 4, respectively. The corresponding RF frequencies and peak dee voltages are shown in tab. 1. For each of the four test ions the calculated,  $f_{\text{RF,calc}}$ , and nominal,  $f_{\text{RF,nom}}$ , RF frequencies, as well as the maximum deviation of orbital frequencies due to the fluctuations of the given magnetic fields are given. The nominal orbital frequency is the one used as an input in the isochronous magnetic field calculation. Also given are the harmonic number,  $h$ , and the amplitude of the acceleration RF voltage,  $V_{\text{p,RF}}$

**Table 1. Orbital frequencies**

	H	H <sub>2</sub> <sup>+</sup>	<sup>4</sup> He <sup>+</sup>	<sup>40</sup> Ar <sup>6+</sup>
$h$	1	2	3	4
$V_{\text{p,RF}}$ [kV]	75	70	65	65
$f_{\text{RF,nom}}$ [MHz]	20.037	28.019	20.714	18.168
$f_{\text{RF,calc}}$ [MHz]	20.058	28.0234	20.7033	18.1652
$\Delta f$ [%]	0.065	0.045	0.040	0.025

## METHOD DESCRIPTION

The charged particle motion inside a cyclotron may be described by the following equations:

$$\frac{d\mathbf{r}(t)}{dt} = \frac{1}{m_0} \sqrt{1 - \frac{v(t)^2}{c^2}} \mathbf{p}(t) \quad (1)$$

and

$$\frac{d\mathbf{p}(t)}{dt} = \frac{q}{m_0} m_0 \mathbf{E}(t, \mathbf{r}) + \sqrt{1 - \frac{v(t)^2}{c^2}} \mathbf{p}(t) \times \mathbf{B}(\mathbf{r}) \quad (2)$$

where  $\mathbf{r}$  represents the position of the particle,  $\mathbf{p}$  is the momentum and  $v$  is the velocity intensity. The rest-mass of the particle is  $m_0$ ,  $q$  is the electric charge and  $c$  is the speed of light. The electric field inside the cyclotron is  $\mathbf{E}$  and magnetic induction is  $\mathbf{B}$ .

An algorithm with the adaptive time step is proposed for tracking beam trajectories in the accelerating region. The previously developed computer code for the extraction region utilized the fourth order Runge-Kutta ODE integration scheme. It is often used in problems of trajectory tracking for its simplicity, good accuracy, as well as stability. With-

out the adaptive time step, however, it would result in intolerably long computation times and, consequently, in an insufficient accuracy. Thus, the above equations are solved using the adaptive time step Runge-Kutta method of the fourth order. The chosen time steps have to comply with the two accuracy requirements – the local position calculation error must not exceed the required maximal position error,  $x_{\text{err}}$ , while the local error of the momentum calculation must not be greater than the maximal momentum error,  $p_{\text{err}}$ , given as a fraction of the initial momentum. In addition to the described main procedure, other changes have been made and a set of auxiliary procedures has been developed.

Magnetic field maps used as an input give the values of the magnetic induction in the median plane with the radial resolution of 1 cm and angular resolution of 1°. The magnetic induction and its derivatives at an arbitrary point in the median plane are calculated using the linear interpolation of the values in the four surrounding grid points. The magnetic induction outside the median plane is determined using  $\mathbf{B} = 0$ ,  $\nabla \cdot \mathbf{B} = 0$ , Taylor's expansion of the second order, and numerical derivatives of the magnetic induction in the median plane (the central difference formulas of the fourth order). The electric field can be calculated by means of an analytical approximation, or numerically, using electric field maps. The latter is similar to magnetic induction calculations just described; it is better than the analytical approximation, but requires previously calculated electric field maps. An electric field calculated using the analytical approximation [7] is only valid in the acceleration region. Due to the current unavailability of electric field maps, analytical approximation of the electric field inside the accelerating RF gaps is used. Note that the electric field outside the four accelerating gaps is taken to be zero. The utilization of the numerically calculated electric field maps as an input would enable the application of the code to central region beam dynamics.

The level of isochronism of the given magnetic field maps is evaluated in order to determine the optimal RF frequencies. This analysis is done prior to the utilization of the field maps in beam dynamics calculations. It is intended to check the extent of magnetic field fluctuations which originate, partially, from the imperfections in machining and assembling of the cyclotron magnet parts but, for the most part, from the discrete number of ten trim coils used to adjust the isochronized fields to their calculated ideal values. Orbital frequencies are calculated for a number of static equilibrium orbits (SEO) for each of the magnetic fields. The one to one correspondence between the equilibrium orbit, ion energy, and mean orbit radius is used to represent the results, as the dependence of the ion gyration frequency on the mean equilibrium orbit radius. The optimal RF frequency for the beam in

question is then calculated as an average orbital frequency in the user-defined range of radii, multiplied by the harmonic number. These adjusted RF frequencies often yield better results in beam dynamics than the nominal values.

The initial coordinates of the central ion in a test beam are estimated and the other test ions in a beam randomly generated around it, because the actual data regarding the central region beam dynamics was unavailable. Obviously, the data used as an input for the accelerating region beam dynamics simulations should be obtained from the central trajectory data and beam emittances around it resulting from the central region beam dynamics simulations. Instead, the central ion could be taken to be the one traveling along the accelerated equilibrium orbit (AEO). However, finding the accelerated equilibrium orbit is a complex and time consuming optimization problem. Secondly, there is not much use for acceleration region trajectory tracking corresponding to optimal acceleration, if it is not matched to actual central region particle trajectories. Even a small offset in the central ion orbit centering can yield significantly different simulation results. In the future, the AEO will be studied by means of an optimization procedure, in order to determine how far from the optimal is the achieved acceleration.

For the time being, the initial central trajectory starting point is, in the first approximation, taken to be on the static equilibrium orbit. The tracking of the trajectory is performed from the chosen initial point to the given final radius and azimuth of the extraction stripping foil. In order to obtain results which would be realistic at least to some extent, the information on energy gain is used to evaluate the motion of the centers of the curvature barycenter. The result is used to further adjust the starting point position, through an iterative process, in order to minimize the distance between the center of the curvature barycenter and the machine center. Since part of the input data is estimated rather than taken from the real central region simulation output, the results obtained are not expected to be fully realistic. However, the aim is to establish the simulation procedure and check the operation of the newly developed software

Finally, the trajectories corresponding to a number of ions around the central ion that represent the beam are simulated and the data is recorded in time steps corresponding to those of the central ion trajectory.

## RESULTS

As an illustration of trajectory tracking analysis, the behavior of the four referent ion beams is an-

alyzed. These are  $H^-$ ,  $H_2^+$ ,  $^4He^+$ , and  $^{40}Ar^{6+}$ . Different acceleration regimes of the VINCY Cyclotron use the harmonic numbers ranging from one to four. Acceleration regimes with the harmonic numbers 1, 2, 3, and 4 are used to accelerate  $H^-$ ,  $H_2^+$ ,  $^4He^+$ , and  $^{40}Ar^{6+}$  test ions, respectively. Note that the  $^4He^+$  ion beam can also be accelerated using the harmonic number  $h = 4$ . The final extraction energies for these ions are expected to be 65 MeV for  $H^-$ , 30 MeV per nucleon for  $H_2^+$ , 7 MeV per nucleon for  $^4He^+$ , and 3 MeV per nucleon for  $^{40}Ar^{6+}$ .

The acceleration mechanism in an isochronous cyclotron is based on the synchronization between particle gyration and electric field frequency. Ideally, the isochronous magnetic field should provide constant gyration frequency of a test ion, while in reality, the smaller the deviation of the gyration frequency, the better. The frequency of the RF resonators should be equal to or a multiple of the ion orbital frequency. Therefore, for each of the isochronous fields corresponding to the four test ions, the dependence of orbital frequency on ion energy is investigated. The orbital frequency of a test ion is calculated for a number of static equilibrium orbits, denoted by corresponding ion energies. The ion energy increment is taken to be 0.5 MeV. The optimal RF frequency for the beam in question is then calculated as an average orbital frequency in the user-defined range of radii, multiplied by the harmonic number. The radial range from 300 mm to 840 mm is chosen because it corresponds to the acceleration region. Radii smaller than 300 mm correspond to the central region area. The upper limit of 840 mm is equal to the extraction radius.

Plots of the calculated orbital frequencies *vs.* the average orbital radii and relative orbital frequency offset from an optimal frequency estimate for  $H^-$  and  $H_2^+$  ions are given in fig. 1 and fig. 2, respectively. The results for all four test ions are summarized in tab. 1. The orbital frequencies that correspond to different radii fluctuate around the mean value. This is to be expected, as the isochronized magnetic fields are obtained by adjusting the values of the ten trim-coil currents. Still, we get a good agreement between the estimated and nominal frequencies.

Initial coordinates of the central ions are on the static equilibrium orbits corresponding to the initial kinetic energies of 7.5 MeV, 7.5 MeV, 3.5 MeV, and 15.0 MeV for  $H^-$ ,  $H_2^+$ ,  $^4He^+$ , and  $^{40}Ar^{6+}$  ions, respectively. These energies correspond to the equilibrium orbits with the average radii of about 300 mm. Accuracy requirements for particle trajectory tracking calculations are set to  $x_{err} = 1 \mu m$ ,  $p_{err} = 2 \text{ ppm}$ .

The particle trajectory tracking procedure is executed from the estimated initial point to the extraction radius  $R_{ex} = 84 \text{ cm}$ . The data obtained for the four test beams is summarized in tab. 2, where

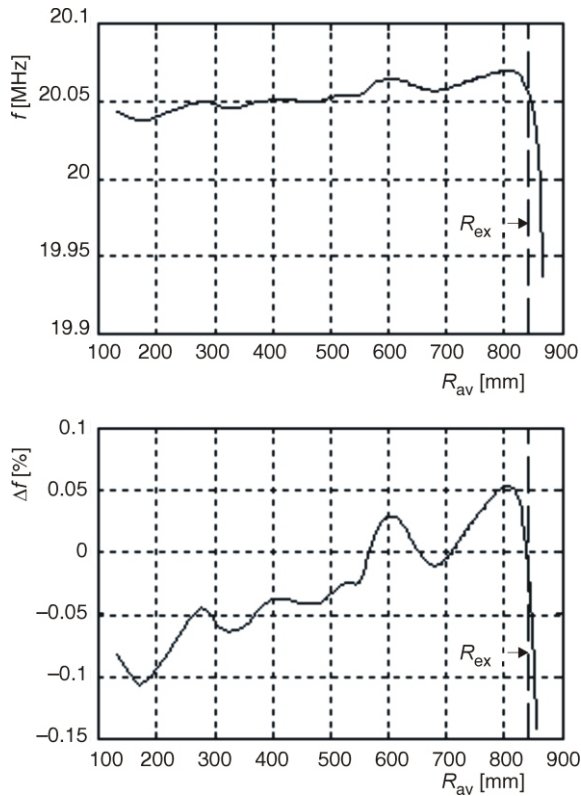


Figure 1. Orbital frequencies vs. average orbital radii (upper plot) and their difference from an average frequency estimate (lower plot), for  $H^-$  ion

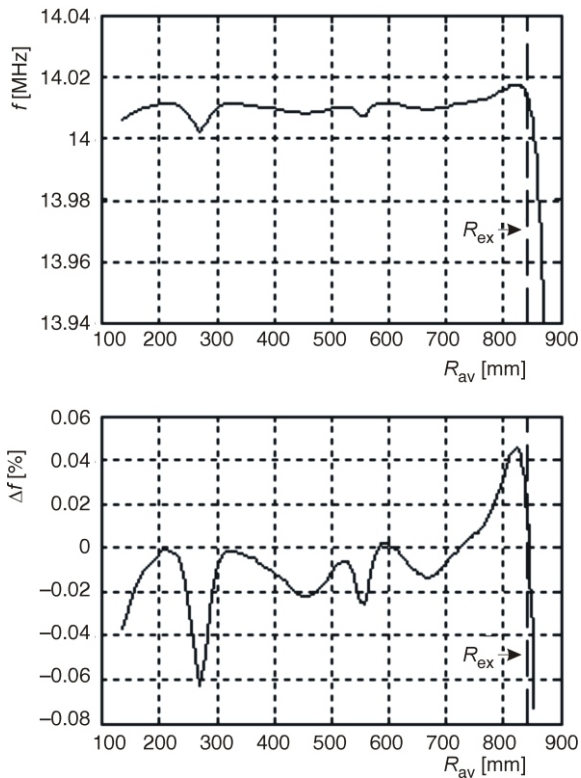


Figure 2. Orbital frequencies vs. average orbital radii (upper plot) and their difference from an average frequency estimate (lower plot), for  $H_2^+$  ion

Table 2. Summary of simulation results

	$H^-$	$H_2^+$	$^4He^+$	$^{40}Ar^{6+}$
$\Delta t$ [ $\mu s$ ]	61.27	36.43	22.31	19.54
$T/A_{nom}$ [MeV/n]	65	30	7	3
$T/A_{calc}$ [MeV/n]	64.40	29.74	6.95	2.98

$t$  is the time the central particle spends traveling along the simulated orbit and  $T/A_{calc}$  is the final kinetic energy.

Nominal extraction energies,  $T/A_{nom}$ , are also given for comparison purposes with our simulation results. Good agreement between these two sets of data is observed. Plots of the median plane central ion trajectory and typical energy increments pattern are shown in fig. 3 and fig. 4, respectively, for the  $^{40}Ar^{6+}$  ion. The trajectories and energy increments for other ions look similar to these, except for larger radii, where the separated orbits cease to be observable, as in the case of  $^{40}Ar^{6+}$ . The orbits become denser and more overlapping as the radius increases.

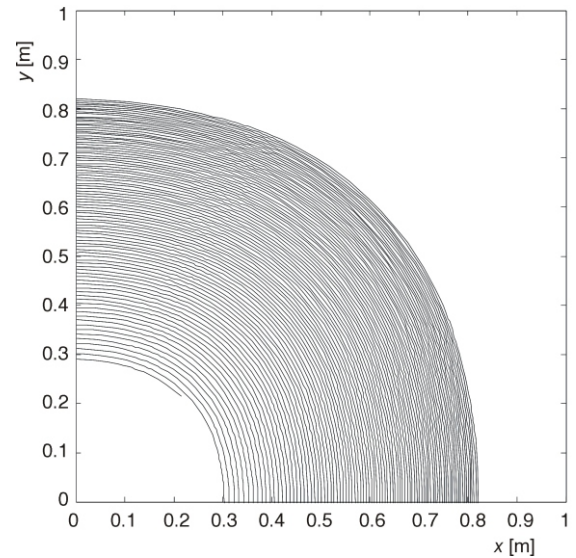


Figure 3. A quarter of the median plane trajectory for  $^{40}Ar^{6+}$  central ion

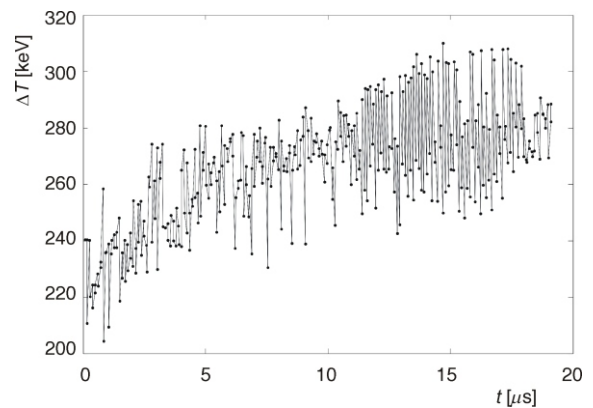


Figure 4. Kinetic energy increments for  $^{40}Ar^{6+}$  central ion



As examples of beam simulation, the radial and axial motions for several ions are shown in fig. 5 and fig. 6. Detailed analysis of beam emittances and acceleration region acceptances is ongoing.

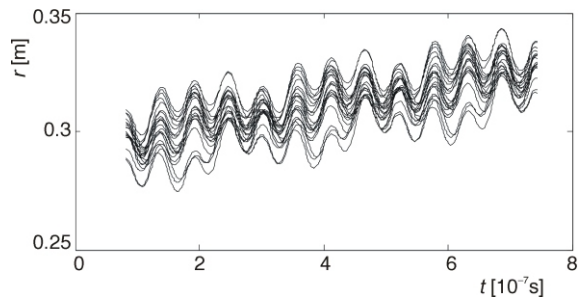


Figure 5. Radial motion for the first three turns for twenty-one  $^{40}\text{Ar}^{6+}$  ions

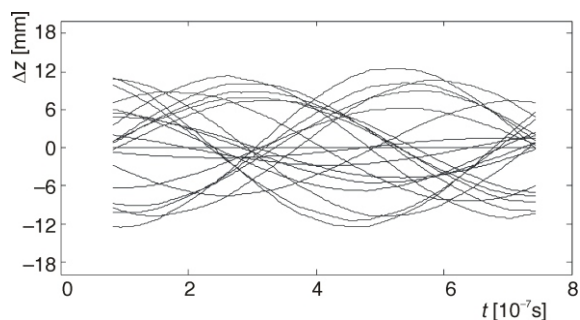


Figure 6. Axial motion for the first three turns for twenty-one  $^{40}\text{Ar}^{6+}$  ions

## CONCLUSION

Problems typical of acceleration region beam dynamics simulation and analysis were addressed. We have described the computer code developed for this purpose and explained several steps that were used to obtain relevant data. The results of the anal-

ysis for the four test beams have been presented as an illustration of beam dynamics analysis. We have shown that the magnetic fields, used as input, have been well designed.

## REFERENCES

- [1] Ristić-Djurović, J. L., Nešković, N., Čirković, S., Compound Particle Tracking Algorithm: Application to the Foil Stripping Extraction System Design, *Proceedings, 6<sup>th</sup> International Computational Accelerator Physics Conference*, Darmstadt, Germany, September 11-14, 2000
- [2] Ristić-Djurović, J. L., Čirković, S. T., Košutić, Dj., Beam Stripping Extraction from the VINCY Cyclotron, *Nuclear Technology & Radiation Protection*, 21 (2006), 1, pp. 21-28
- [3] Nešković, N., Ristić-Djurović, J., Vorozhtsov, S. B., Beličev, P., Ivanenko, I. A., Čirković, S., Vorozhtsov, A. S., Bojović, B., Dobrosavljević, A., Vujović, V., Čomor, J. J., Pajović, S. B., Status Report of the VINCY Cyclotron, *Nukleonika*, 48 (2003), suppl. 2; *Proceedings, XXXIII European Cyclotron Progress Meeting*, Warsaw and Krakow, Poland, September 17-21, 2002, pp. s135-s139
- [4] Čirković, S., Ristić-Djurović, J., Milošević, M., Calculation of the Test Ion Isochronous Field Based on the Measured Magnetic Fields, *Proceedings, 6<sup>th</sup> International Computational Accelerator Physics Conference*, Darmstadt, Germany, September 11-14, 2000
- [5] Čirković, S., Ristić-Djurović, J. L., Vorozhtsov, A. S., Vorozhtsov, S. B., Calibration of the Simulation Model of the VINCY Cyclotron Magnet, *Nuclear Technology & Radiation Protection*, 17 (2002), 1-2, pp. 13-18
- [6] Dubrovin, N. A., Simonov, E. A., Vorozhtsov, S. B., MERMAID 3D Code in ATLAS Applications, ATLAS Note ATL-TECH-2001-003, CERN, Geneva, 2001
- [7] Hazewindus, N., van Niewland, J. M., Faber, J., Leistra, L., The Magnetic Analogue Method as Used in the Study of a Cyclotron Central Region, *Nucl. Instr. and Meth.*, 118 (1974), p. 125

Анђелија Ж. ИЛИЋ, Јасна Љ. РИСТИЋ-ЂУРОВИЋ, Саша Т. ЂИРКОВИЋ

### ПРЕЛИМИНАРНИ РЕЗУЛТАТИ ПРАЋЕЊА ЈОНА У УБРЗАВАЈУЋЕМ РЕГИОНУ ЦИКЛОТРОНА ВИНСИ

У акцелерационом региону циклотрона број обрта јона је велики; стога, праћење јонских трајекторија захтева не само брз прорачун, већ и велику рачунску прецизност. Са тим циљем развијен је програм заснован на методи Рунге-Кута четвртог реда са адаптивним кораком интеграције. Адаптивни корак интеграције одређује се тако да буде постигнута задата тачност како положаја тако и импулса честице. Као улазни податак користе се магнетска поља, која су претходно испитана са становишта своје изохроности, односно радијалних флукуација орбиталних учестаности. Трајекторије су прорачунате за четири тест јона:  $\text{H}^-$ ,  $\text{H}_2^+$ ,  $^4\text{He}^+$  и  $^{40}\text{Ar}^{6+}$ .

Кључне речи: циклојрон, јонски сноп, прорачун трајекторија, адаптивни корак интеграције, магнетска поља, изохроности